JTTEE5 17:115–123
DOI: 10.1007/s11666-007-9144-2
1059-9630/$19.00 © ASM International

Application of Suspension Plasma Spraying (SPS) for Manufacture of Ceramic Coatings

Holger Kassner, Roberto Siegert, Dag Hathiramani, Robert Vassen, and Detlev Stoever

(Submitted February 22, 2007; in revised form May 24, 2007)

Conventional thermal spray processes as atmospheric plasma spraying (APS) have to use easily flowable powders with a size up to 100 μm. This leads to certain limitations in the achievable microstructural features. Suspension plasma spraying (SPS) is a new promising processing method which employs suspensions of sub-micrometer particles as feedstock. Therefore much finer grain and pore sizes as well as dense and also thin ceramic coatings can be achieved. Highly porous coatings with fine pore sizes are needed as electrodes in solid-oxide fuel cells. Cathodes made of LaSrMn perovskites have been produced by the SPS process. Their microstructural and electrochemical properties will be presented. Another interesting application is thermal barrier coating (TBC). SPS allows the manufacture of high-segmented TBCs with still relatively high porosity levels. In addition to these specific applications also the manufactures of new microstructures like nano-multilayers and columnar structures are presented.

Keywords coatings for gas turbine components, fuel cells, nanostructured materials, new structures, segmented coatings, suspension plasma spraying

1. Introduction

Nano-materials are widely used in different fields of application because of the improved mechanical and physical properties of the materials and produced units. The manufacture of nanostructural coatings often involve thin film processes like physical vapor deposition (PVD), chemical vapor deposition (CVD), sol-gel deposition or laser-based processes. These processes lead to coatings with very good mechanical and physical properties. The main disadvantages of these processes are the slow application speed and the high process costs. Another possibility to produce coatings is the thermal spraying, in which particles typically in the micrometer range are molten and deposited on a substrate. Compared to the thin film processes, the coating structure, especially of ceramics, is more complex and full of defects like pores and microcracks. However, the application speed is much higher and the process costs are much lower. (Ref 1-13). An often applied thermal spray process is the atmospheric plasma spraying (APS) in which flowable powders with a typical size range between 10 and 100 μm are used as starting material. Nano-scaled powders cannot be directly used in this process due to their low flowability. This leads to a limitation of the resulting splat size and the achievable microstructure. One possible method to process nano-scaled particles is the use of agglomerated nano-powders. But these agglomerates have a size from 10 to 200 μm. In contrast, the suspension plasma spraying (SPS) process often uses a suspension of submicron powders to inject the coating material into the plasma torch. So nano-particles dispersed in a suspension can directly be injected into the plasma torch. Figure 1 shows micrographs of a typical flowable spray powder (Sulzer Metco AG, Wohlen, Switzerland) and an agglomerated powder (Inframat Corporation, Farmington, CT) used in the APS process compared to nano-particles (Treibacher AG, Althofen, Austria) used in the SPS process. Another alternative is the use of precursor liquids for the plasma spraying with fluids. Therefore, a chemical precursor is injected into the plasma jet. Due to physical and chemical reactions, the desired ceramic is generated in the plasma (Ref 14, 15).

Holger Kassner, Roberto Siegert, Dag Hathiramani, Robert Vassen, and **Detlev Stoever**, IEF-1, Forschungszentrum Jülich GmbH, Juelich Germany. Contact e-mail: h.kassner@fz-juelich.de.

2. Experimental

The plasma-sprayed coatings were produced with different plasma guns all supplied by Sulzer Metco AG, Wohlen, Switzerland. In sum, three different plasma guns were used, a one-cathode F4 APS torch, a three-cathode Triplex I APS torch, and a three-cathode Triplex II APS torch. All plasma guns were mounted on five- or six-axis robots. Austenitic steel served as substrate material. The dimension was a square with a side length of 50 mm and a thickness of 2 mm. All substrates were sand-blasted before coating. For the thermal barrier coatings, a partial yttria-stabilized zirconia (5YSZ) from two companies was used. The first 5YSZ powder was from Tosoh Corporation, Tokyo, Japan with a particle diameter of $d_{50} = 300$ nm. The other one was from Treibacher AG, Althofen, Austria with a particle size of $d_{50} = 25$ nm. The fully stabilized YSZ powder was from Praxair GmbH, Ratingen, Germany, ZRO-292 with a particle size

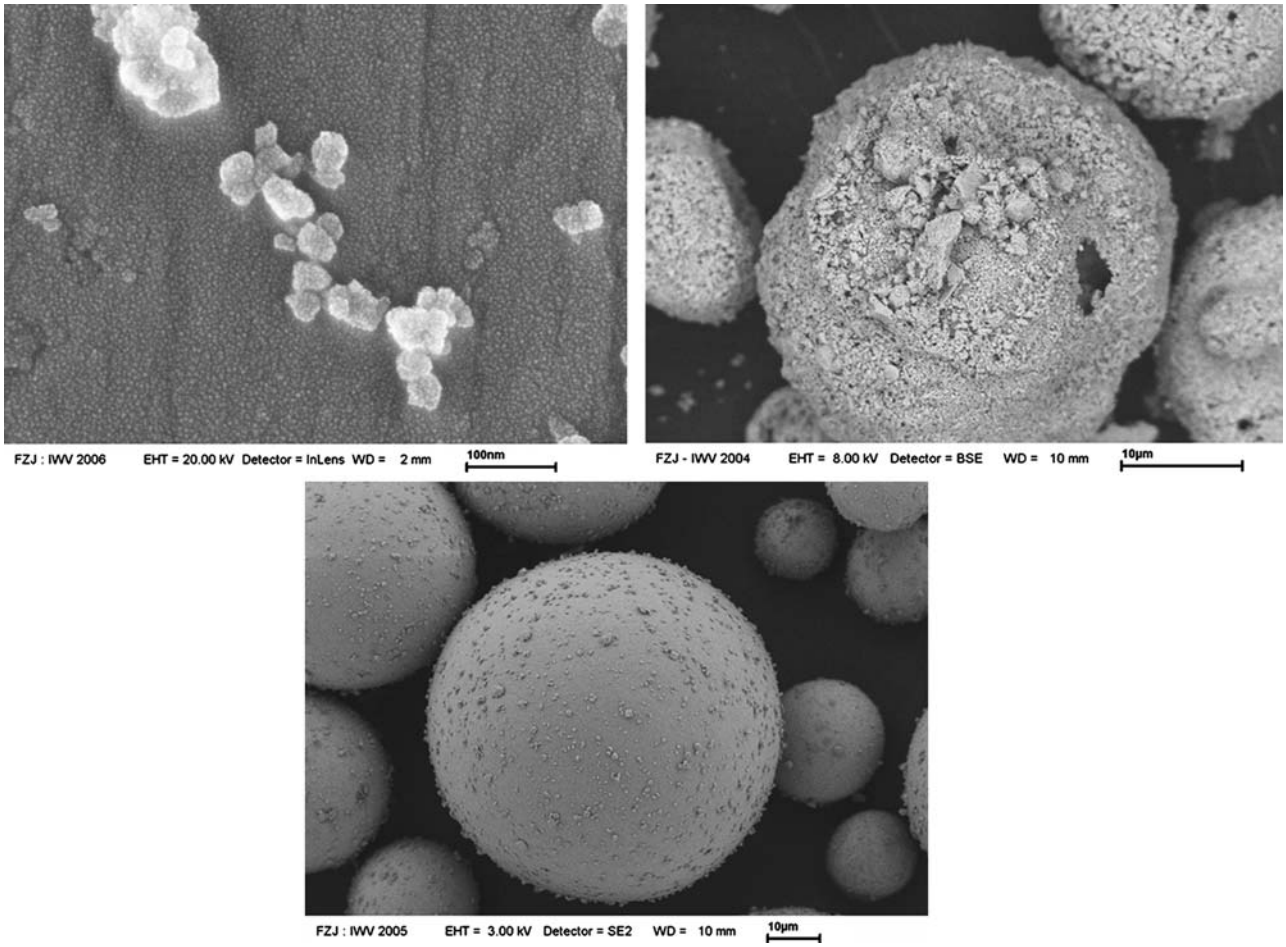

Fig. 1 Particles used in the SPS process (upper, left) agglomerated powder (upper, right) and spherical particle for an APS process (down)

between $d_{10} = 17$ µm and $d_{90} = 83$ µm. For the alumina coating, a powder with a $d_{50} = 1.71$ µm from Martinswerke GmbH, Bergheim, Germany was used. By ball-milling, a particle size of $d_{50} = 500$ nm was achieved. The perovskite powder was a spray-dried $La_{0.65}Sr_{0.3}MnO_3$ powder produced in the Forschungszentrum Jülich, Jülich, Germany with a diameter of $d_{50} = 500$ nm. All powders were dispersed in an ethanol-based suspension. The mass content varied between 10 and 30 wt.%. To achieve the required particle size, all powders were dispersed in ethanol and ball-milled for at least 24 h. As grinding stock, zirconia or alumina balls with a diameter from 2 to 5 mm were used. The suspensions have been stabilized by the addition of 1.5 wt.% of a dispersant. For the APS standard coatings a 5YSZ from Sulzer Metco AG, Wohlen, Switzerland with a diameter of $d_{50} = 50$ µm was used. The temperature was monitored with a 4 M8 pyrometer (Land Instruments GmbH, Leverkusen, Germany) operating with a wavelength from 8 to 14 µm. Particle size and distribution was measured with an Acoustic Spectrometer DT-1200 (Dispersion Technology Inc., Bedford Hills, NY) or an Analysette 22 (Fritsch GmbH, Idar Oberstein, Germany) using Fraunhofer diffraction. The microstructure was inspected in cross sections or freestanding coatings with a scanning electron microscopy (SEM) with energy dispersive microanalyses (EDX). Images of the microstructure were taken using a SEM Leo 1530 (Carl Zeiss NTS AG, Germany) or an Ultra 55 (Carl Zeiss NTS AG, Germany). Phase evolution was observed by x-ray diffraction (XRD) with a D500 (Siemens AG, Germany) diffractometer equipped with diffracted-beam monochromator for Cu-K_α. For porosity measurements, an image analysis (Analysis, Soft imaging systems GmbH, Münster, Germany) and mercury porosimetry (Pascal 140/440, Fisons Instruments, Ismaning, Germany) was used.

3. Results

3.1 YSZ Coatings Produced by SPS

Typically the molten powders in the APS process generate splats with a diameter of up to a few hundred and a thickness of several micrometers. As remarked, the SPS uses sub-micron particles with a size from 20 nm up to a few hundred nm. Thus, splat sizes from 0.2 to 6 µm with a

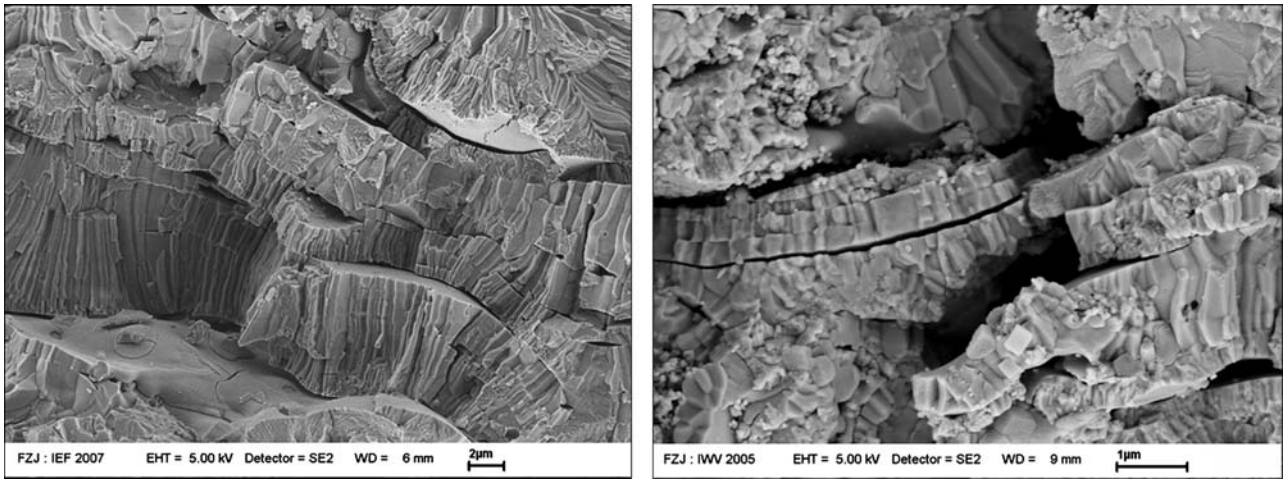

Fig. 2 5YSZ structure of a conventional APS coating (left) and a SPS coating (right)

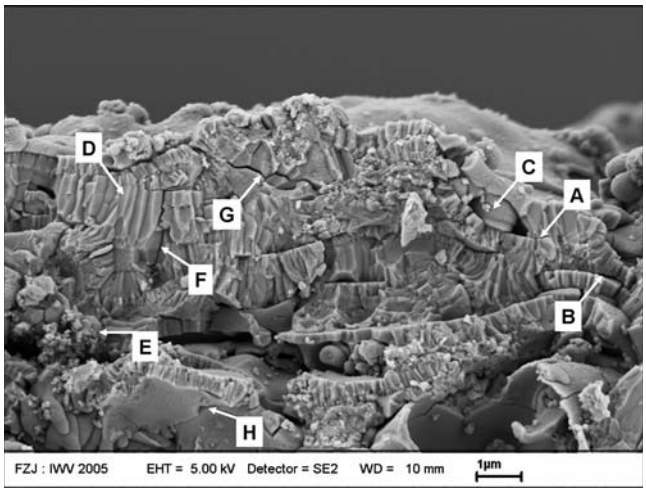

Fig. 3 Main fracture features of a SPS coating

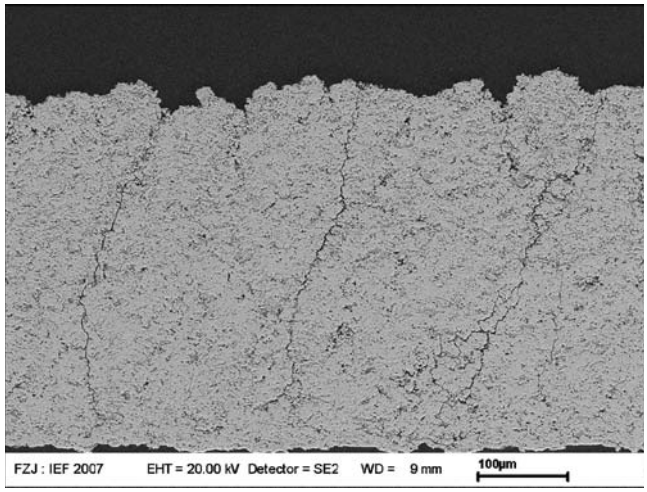

Fig. 4 Cross section of a 5YSZ SPS coating with segmentation cracks

splat thickness of 20-300 nm are obtained (Ref 3, 10, 16, 17). This results in an increased number of lamellas in the coating. Figure 2 shows the transverse fracture surface of a standard APS coating and a SPS coating. Both coatings were produced with 5YSZ using a Triplex I gun.

The standard coating shows a lamellar structure with a mean thickness of about 2.5 µm. Compared to this, the SPS coating has an increased number of lamellas. The mean lamella thickness is about 250 nm (Ref 16). Due to the increased cooling rate, also the trans-splat grains in the SPS splats are much higher than in an APS splat.

Several important structural features of a SPS coating are shown in Fig. 3. A 10 wt.% ethanol-based suspension containing 5YSZ (Tosoh Corporation) and a Triplex I plasma gun were used. Seven different features are indicated in the figure. Compared to APS structures there are more and thinner lamellas formed by single splats. As in standard coatings, SPS coatings show areas of good (A) and poor (B) inter-splat bonding. The SPS lamellas also contain fine-grained so-called overspray particles (E) and re-solidified particles (C). The splats have a columnar grain growth (D) with a grain thickness up to 0.1 µm. There are also some inter-lamellar cracks (G). Another difference is the increased number of microcracks (H) in the single splat and the high number of intrasplat cracks (F) in the coating.

Using a lower magnification, additional new features can be found compared to conventional APS coatings. Figure 4 shows segmentation cracks in a free-standing 5YSZ coating (Treibacher AG) produced with a 10 wt.% ethanol-based suspension and a Triplex II gun. The segmentation crack density of is about 7 cracks/mm. Conventional plasma spraying also allows the manufacture of coatings with segmentation cracks. This type of coatings is often used as thermal barrier coating. However, in APS coatings a very dense microstructure is essential for the generation of these segmentation cracks. In addition, the

achievable crack densities in most cases are below 5/mm. In contrast, the SPS process allows higher segmentation crack densities and the coating microstructure is still rather porous. This combination of features is ideal for an application as thermal barrier coating as it allows a good thermal insulation due to the high porosity and a strain tolerance as a result of the segmentation cracks. Investigations on the performance of these new SPS TBCs are now under way.

3.2 SPS for SOFC

Another interesting field for the implementation of the SPS technology is the manufacture of high-performance solid oxygen fuel cells (SOFC). Fuel cells enable the conversion of chemical energy directly into electrical one with high electrical efficiency. However, the main reasons that the SOFC is not a commercial product yet are the high production costs combined with high degradation rates or low performance. So the main targets of SOFC development are to reduce the costs and increase the performance. Thermal spray processes might have the potential of cost reductions. So APS, especially the SPS process seems to be an attractive technique for generating high-performance cathodes combined with low production coasts. To afford this, it is necessary to raise the amount of triple-phases boundaries where the cathodic oxidation reaction occurs. Therefore, a large and homogenous active area of an ionic and an electronic conductor including pores within the CFL has to be produced. An often used material mixture is a perovskite, an electronic conductivity and fully Y_2O_3-stabilized zirconia (YSZ) as ionic conductor. In the present article a LSM ($(La_{0.65}Sr_{0.3})MnO_3$) perovskite and YSZ (Praxair GmbH) is used. Compared to the conventional APS process, SPS allows a much higher amount of triple-phase boundaries due to the much smaller particle size. This should lead to a higher amount of triple-phase boundaries which are essential for a high performance. A reaction between the different materials during deposition has to be avoided.

3.2.1 Cathode Functional Layer (CFL) by SPS Processes. Basically two different processes are capable to produce a CFL by the SPS process. A single injection of a mixed suspension or a separate injection of two single-phase suspensions could be made. Figure 5 shows the injection of the two suspensions. The angle between the injectors for the two suspensions is 120°.

For both processes, stabilized ethanol-based suspensions with a mass content of 30 wt.% were used. The suspension for the single injection contains a mix of LSM and YSZ particles with a mass ratio of 50:50. Two different suspensions were applied for the separate injection. One suspension only contains YSZ, the other only LSM particles. In order to find the better of the two SPS processes, different tests have been carried out including an electrochemical performance test. The other components of the SOFC were produced in an equal way. An optimal CFL should have a lot of triple-phase boundaries and the two phases should exist separately. A reaction between the ceramics should be avoided.

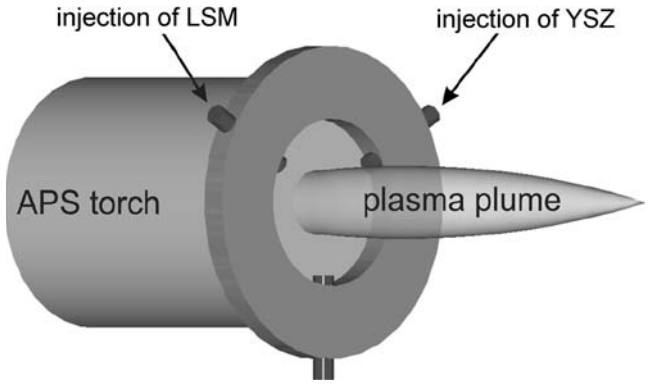

Fig. 5 Injection of the two separate suspensions

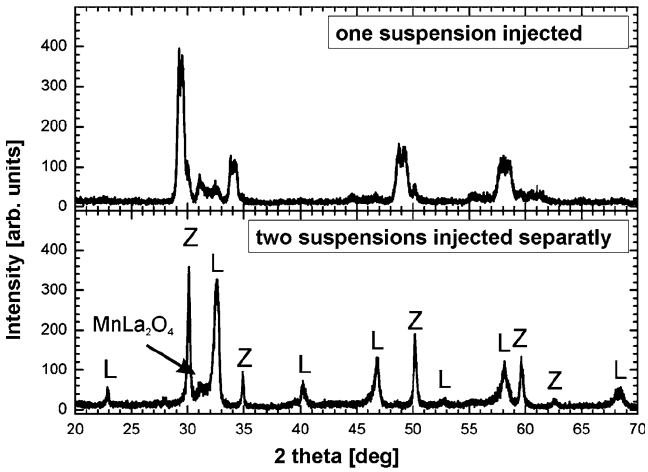

Fig. 6 X-ray diffraction patterns of the SPS coatings. Top: Single injection of a combined LSM/YSZ suspension. Bottom: Separate injection of LSM and YSZ. L and Z labels LSM and YSZ

3.2.1.1 Single Injection: As the XRD measurement in Fig. 6 shows that a reaction took place for the mixed suspensions during deposition. The diffraction diagram shows only a main phase with a cubic structure. This structure belongs to an intermediate phase, located between YSZ and La_2ZrO_7. This can be explained by the fact that the mixed suspension contains a mixture of LSM and YSZ. After fragmentation, vaporization, and fusion, the molten droplets contain a material mix. As the melt will be formed out of the two ceramics during the solidification, a mixed phase is formed. So it is not possible to achieve separate phases by a single injection.

3.2.1.2 Separate Injection: As remarked, two single-phase suspensions were used for the separate injection. In contrast to the single injection, the XRD pattern (Fig. 6 bottom) of the separate injection shows the cubic YSZ and perovskite LSM. There is only a small peak between the two main peaks which belongs to $MnLa_2O_4$. The decomposition of the LSM could be reduced by using a smaller

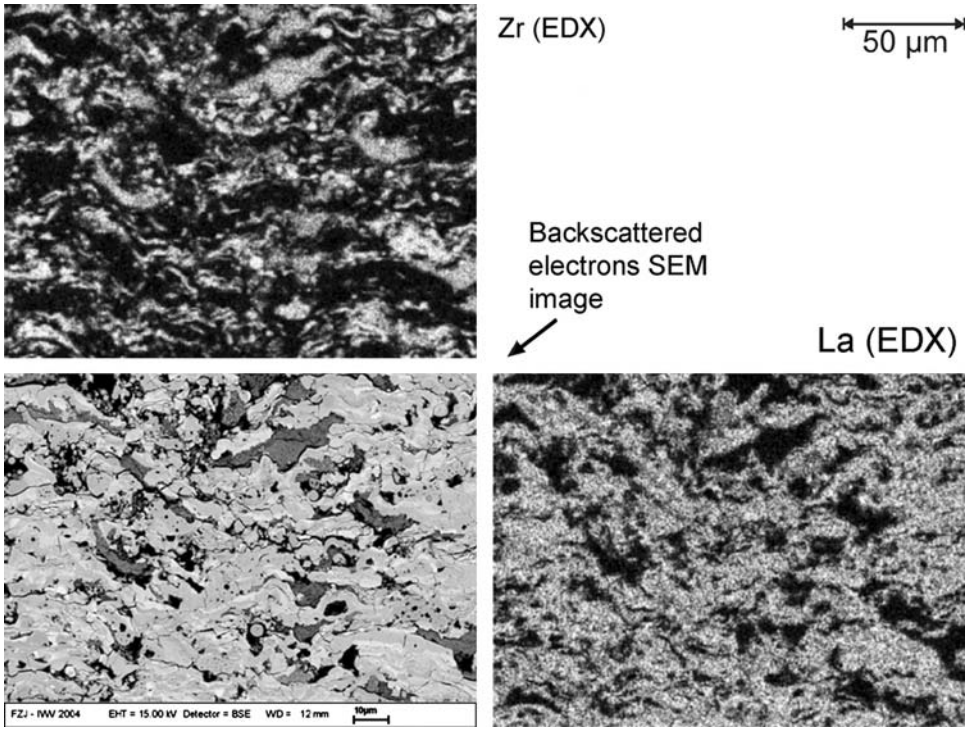

Fig. 7 Cross section of a SPS coating by separate injection of LSM and YSZ into the plasma. Top: Zr-L mapping. Lower left: BSE image. Lower right: La-Lα mapping

thermal load of the plasma. Figure 7 illustrates the typical structure of a coating produced by a separate injection.

The backscattered electron (BSE) image shows a phase size lower than 1 µm. This is much smaller compared to microstructures produced by the conventional APS process. Also areas containing clusters of unmolten particles, also known as ''overspray,'' can be seen. The EDX mappings are taken in the same area. The porosity of the coating is about 40%. A voltage vs. current curve of samples containing a CFL prepared by the separate injection is shown in Fig. 8. The area-specific resistance of the system was −1.3 Ω cm^2. At a cell voltage of 700 mV, a current density below 200 mA/cm^2 is obtained. So the power density is about 120 mW/cm^2 demonstrating the possibility to produce SOFC cathodes by the SPS technique. However, the values are rather low compared to those of sintered cells. A further optimization with respect to homogeneity and grain size has to be made before an application is envisaged.

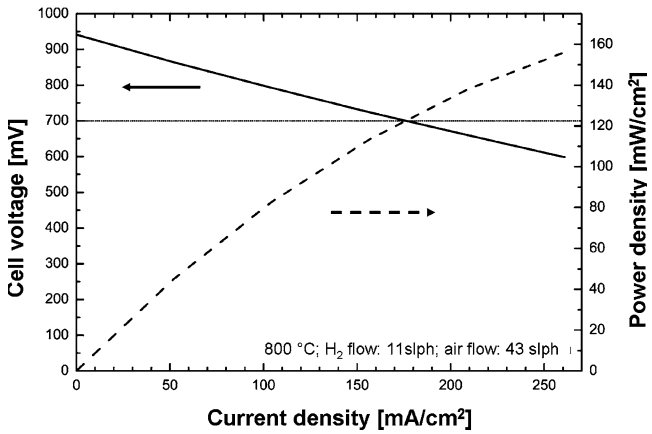

Fig. 8 Voltage vs. current density curve for the SOFC. The CFL was produced by the separate injection of LSM and YSZ

3.3 Future Perspectives for SPS

In the future, another advantage of the SPS process might become more interesting. Compared to the APS process, the SPS process affords it to generate new types of structures. These structures have properties which could not be obtained by any other technique. But also the injection of the suspension could be optimized by new operations.

3.3.1 Two-Phase Atomization. The SPS process is rather sensitive to changes in the process parameters. The method of injecting the suspension is one of the most influencing parameter. In most cases, a single injection is used (Ref 1-4, 14, 15). Often the only changeable parameter is the injection pressure. Thus only the injected mass and the injection speed can be altered. Thereby the injection of the suspension occurs in the form of a jet and so it is not possible to influence the droplet size as it is controlled by the atomization process. As the physical and mechanical behavior of APS coatings depends on the splat size, a direct method to control the droplet size would be desirable. A well-defined droplet size can be achieved by a

well-designed atomizer. A possibility is the use of a two-phase atomizer with a separate gas stream for the atomization process. The big disadvantage of this type of atomizer is the high mass ratio between gas and suspension. Normally a mass ratio of up to 25:1 is necessary to guarantee a stable atomization. This high amount of gas influences the plasma torch by cooling down the plasma. This leads to a reduced fluid vaporization and at least anticipates the melting of the ceramic. To obviate this effect, a new kind of atomizer was designed. The doable droplet size and velocity can be influenced by the gas and suspension pressure. Another disadvantage is the big dimension of the nozzle compared to a single injection nozzle. The former used commercial atomizer form Lechler AG, Metzingen, Germany has a dimension of $36 \times 20 \times 36$ mm. Due to this, it is not possible to use the standard injection bracket or inject at least at the standard injection point. So the injection point moves from near the gun exit up to a few centimeters from the gun exit. This on the one hand leads to a decreased dwell period in the plasma and on the other hand to an injection into the already annealed plasma. Both effects at least impair the coating structure. Moreover, it is impossible to perform an internal injection with these big dimensions. Another problem is the wide angle of the generated spray. Commercial two-phase atomizers are often working with spray angles of up to 60°. Due to this, a high amount of the suspension is sprayed next to the plasma or into the colder regions. Nevertheless these particles which are not molten will be implemented in the coating. This leads to a worse coating structure combined with a low injection efficiency. These big disadvantages are often rightly mentioned as reasons against the use of two-phase atomizers (Ref 3, 4). The new atomizer reduces these disadvantages or cancels them completely. Due to the new design, small droplets could be produced before entering the plasma without affecting the plasma attributes negatively. The fragmentation of 16 gr/min of suspension could be achieved by using only 2 slpm air. At this, a mean droplet diameter from $d_{50} = 15$ to 60 μm could be generated. The commercial atomizer from the Lechler AG, Metzingen, Germany needs more than 25 slpm air for the same amount of suspension, which is also a low level for these types, and generates a droplet diameter of $d_{50} = 50$-100 μm. Also the reduced dimensions of the new atomizer show a lot of advantages compared to a commercial one. The injector diameter is about 3 mm. The circuit points for the suspension and air are located 60 mm away from the injection point. So it is possible to use the standard injection bracket for external injection. Furthermore, it is possible to inject the suspension with different injection angles. Thereby nearly the same injection point as by the normal powder spraying could be reached. The angle of the generated spray is reduced to 15°. So the diameter of the spray pattern is projected less than 2 cm on the centerline of the plasma. Thus the amount of unmolten particles and particles which could not penetrate the plasma was reduced to a negligible level. Figure 9 shows splats of 5YSZ (Tosoh Corporation) fabricated by SPS with the new atomizer compared to conventional APS splats. For both processes, a Triplex II plasma gun (Sulzer Metco AG) was used. For the SPS process, a 20 wt.% ethanol-based suspension was injected. The plasma parameters for both processes were the same. The achievable splat size in the SPS process is up to 20 times lower than in the conventional APS process. Splats from the APS process show a diameter from 30 to 80 μm whereas splat sizes from the SPS process with the new atomizer are from 0.1 to 5 μm. Also the microcrack density from the splat is much higher in the SPS process. The usable mass load for the suspension could be varied up to 30 wt.%. Another advantage is the targeted variation of the coating structure. A wide band of structures and porosities could be obtained by changing the parameters for the gas and suspension injection. For example, the influence of the gas pressure is shown in Fig. 10. A 20 wt.% suspension of PYSZ (Tosoh Corporation) was injected into the plasma torch. All other parameters remained the same. The porosity in the coating could be varied from 15% to more than 50%. The coating structure was also influenced by changing other parameters like the nozzle design, the spraying conditions, and the suspension properties. Figure 11 shows a SEM

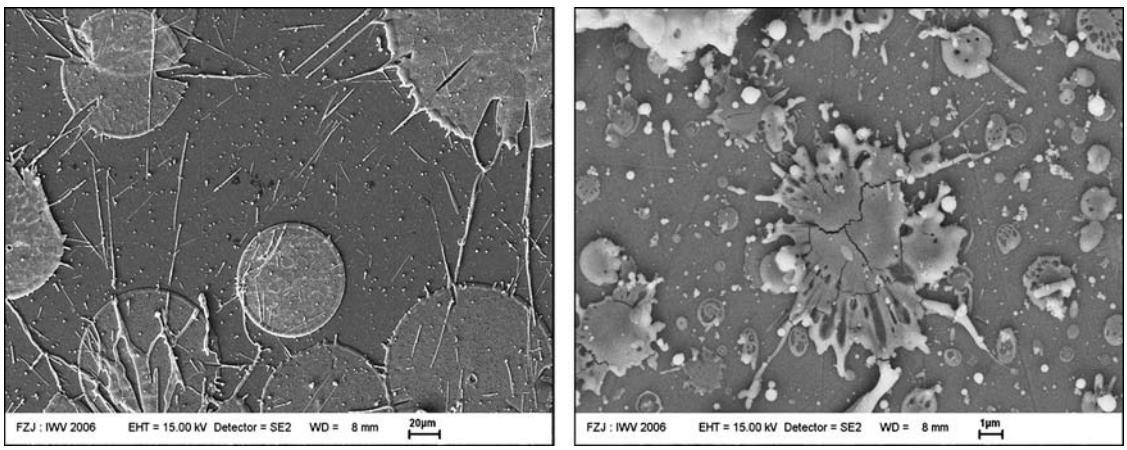

Fig. 9 Splats from an APS process compared to the new SPS process

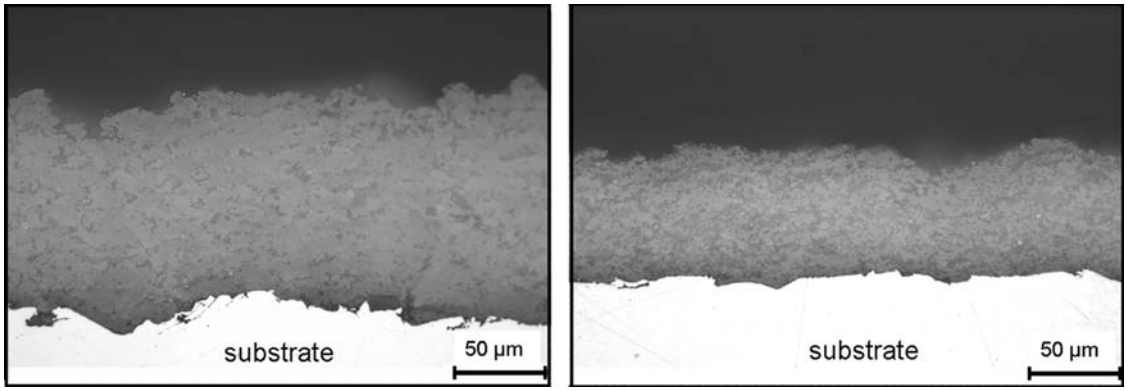

Fig. 10 Influence of the gas pressure on the coating structure: Low gas pressure (left) and High gas pressure (right)

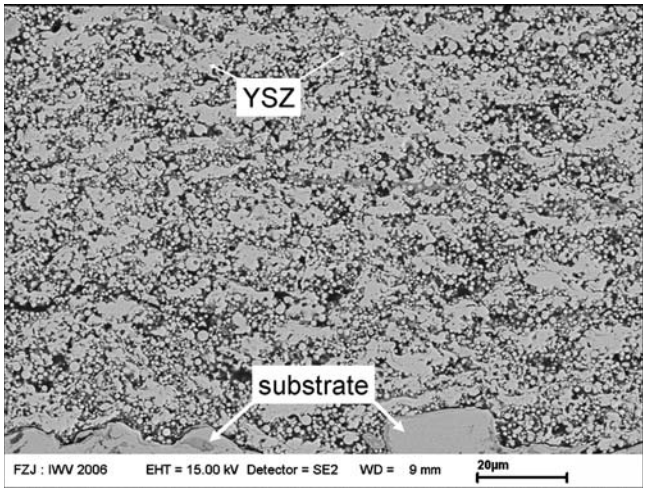

Fig. 11 SEM picture of a coating produced by the improved SPS process

image of a coating produced by a modified ethanol-based 20 wt.% suspension containing 5YSZ (Tosoh Corporation). The porosity resulted in 54%. The plasma parameters were the same as used for the samples of Fig. 10. Another big advantage of the new atomizer is the increased deposition rate which could reach up to 20 µm per cycle.

3.3.2 Columnar Structures. One new type of coating shows a columnar structure. This kind of structure could be produced for alumina and YSZ coatings. Compared to other conventional coatings, this structure shows a distinct difference. Therefore a two-phase atomizer was used to inject the suspension. As plasma gun, a Triplex II gun was used. For the alumina coating, a suspension with 10 wt.% Al_2O_3 (Martinswerke GmbH) dispersed in ethanol was used. The zirconia coatings were sprayed with a 10 wt.% 5YSZ (Treibacher AG). Figure 12 shows SEM pictures of the profile and top view from a freestanding coating with the new structure. During the whole spraying process, the substrate temperature was below 650 °C. The fracture surface of the alumina coating shows a structure with columns. The top view gives a better overview of the structure. The morphology and distance between the single freestanding columns could be influenced by the plasma parameters. The structure of the zirconia on bottom of Fig. 12 was varied only by changing the plasma parameters. The mercury porosimetry gives an open porosity up to 70%.

3.3.3 Nano-Multilayer. Another new structure is a nano-multilayer of two different ceramics. In this case, alumina (Martinswerke GmbH) was mixed with 5YSZ (Tosoh Corporation). A 10 wt.% ethanol-based suspension with a mass ratio of 50:50 was injected. The structure is a fine laminar multilayer with a lamella size from 0.1 to 2 µm, Fig. 13. Some small unmolten particles are embedded in the structure.

4. Conclusion

The SPS process offers a high potential to produce new, fine-grained microstructures. Due to the use of nano-particles, smaller splats can be generated which lead to a high density of fine lamellas. However, to take full advantage of the potential of suspension plasma spraying, an effective injection of the suspension into the plasma plume has to be guaranteed. For the optimization of the injection process, a new type of atomizer was constructed which generates a droplet fragmentation before entering the plasma torch with a droplet size from $d_{50} = 15$ to 60 µm. This is up to 10 times lower compared to an atomizer without using a gas for prefragmentation. Thus the splat thickness could be reduced to values as low as 0.1 µm which is more than 300 times smaller than for conventional plasma spraying. Due to the new design of the two-phase atomizer, the influence of the atomizing gas on the plasma was reduced to a negligible level. The injector dimensions could be reduced to a level which allows the use of standard injection brackets or at least an injection near the normal powder injection point. The small injection angle of the generated spray reduces the amount of unmolten particles in the coating to that of a

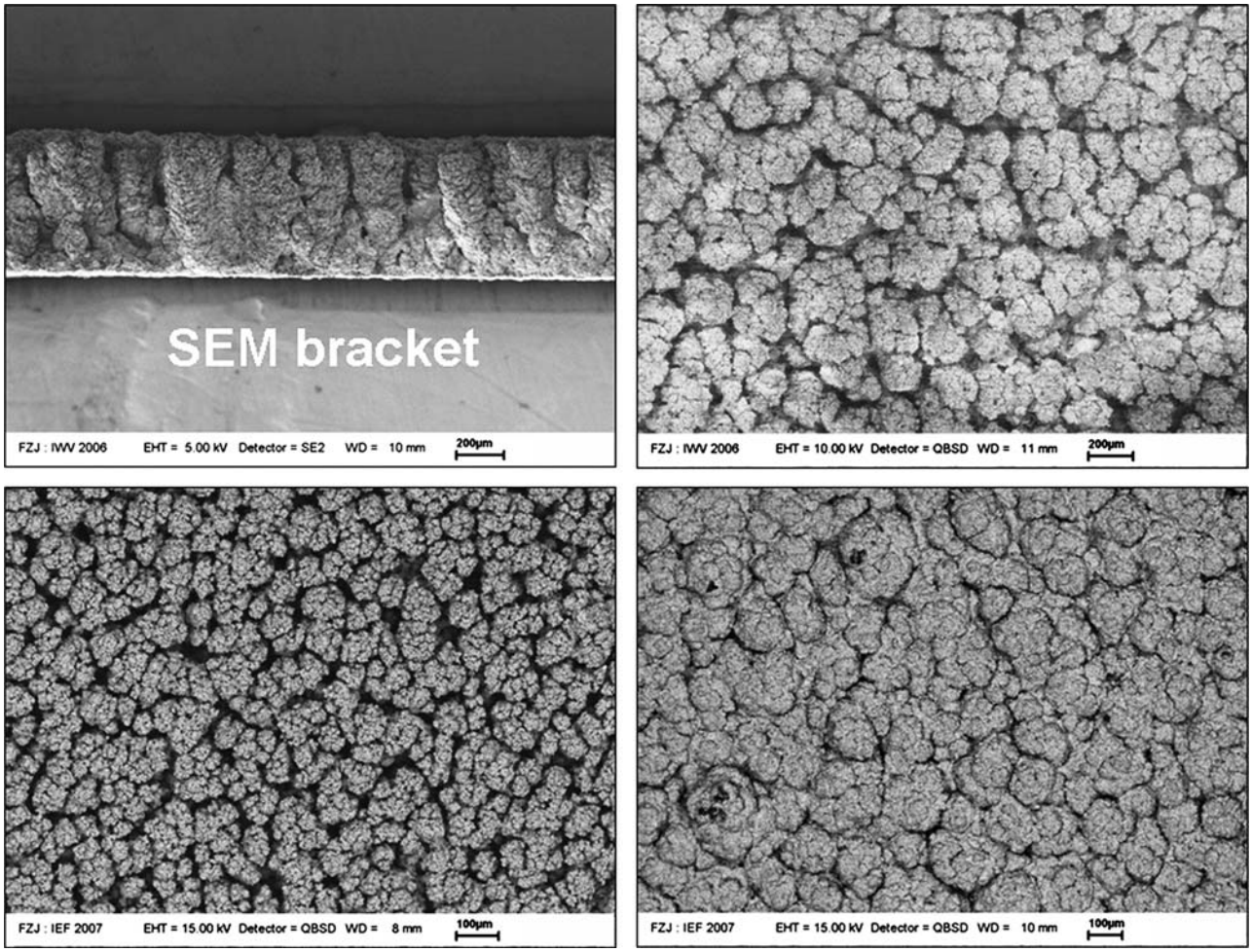

Fig. 12 Fracture surface and top view of the alumina structure (upper left and right). Bottom left and right shows the top view of the zirconia coating

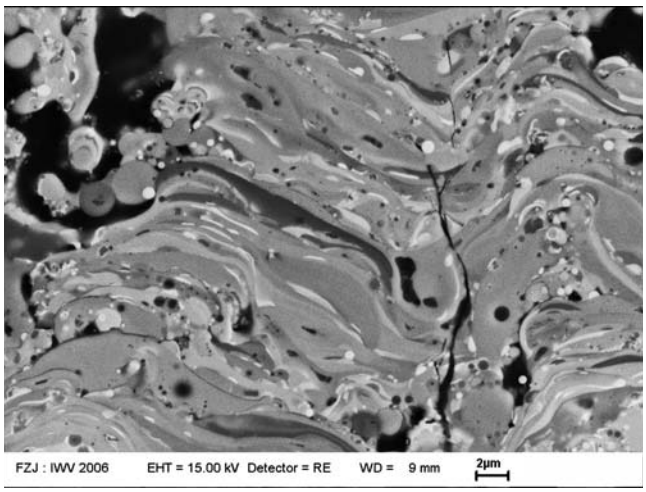

Fig. 13 Nano-multilayer of alumina and zirconia

single injection. The porosity could be controlled in a wide band. The deposition rate was increased up to more than 20 µm/cycle.

With the SPS technology different types of coatings have been produced.

Coatings with a high segmentation crack density of more than 7 cracks/mm can be achieved by appropriate process conditions. This is similar to the values which could be achieved with the precursor plasma spraying (Ref 14, 15). Owing to the increased stress tolerance a high segmentation crack density is very interesting for thermal barrier coatings. The reasons for the high segmentation crack density compared to conventional APS coatings are not yet completely understood. In order to get a better understanding of these mechanisms several tests are running at the moment.

It is possible to deposit two different ceramics without reaction between the two phases using two separate injection ports. As an application of this technology, the deposition of cathode functional layers for solid oxide fuel cells (SOFC) was shown. In addition, the fine porosity level in the cathode layers obtained by SPS technique was essential for this application.

Furthermore, new microstructures could be obtained in the SPS process.

Macroscopically columnar structures with an open porosity of 70% were produced. Combined with the high specific surface, these structures could be interesting for catalytic or separation processes in the chemical industry or in energy systems. Furthermore, nano-multilayers can be generated in which the layer thickness is reduced by several orders of magnitude compared to conventionally sprayed composites. Due to the intense mixing on a nanometer scale it might be possible to generate completely new materials characteristics by using commercial starting ceramics.

References

1. J. Oberste Berghaus, S. Bouaricha, J.-G. Legoux, and C. Moreau, Injection Conditions and In-Flight States in Suspension Plasma Spraying of Alumina and Zirconia Nano-Ceramics, *Thermal Spray 2005: Explore its Surface Potential*!, E. Lugscheider, Ed., May 2-4, 2005 (Basel, Switzerland), ASM International, 2005, p 512-518
2. J. Oberste Berghaus, S. Bouaricha, J.-G. Legoux, C. Moreau, and T. Chraska, Suspension Plasma Spraying of Nano-Ceramics Using an Axial Injection Torch, *Thermal Spray 2005: Explore its Surface Potential*!, E. Lugscheider, Ed., May 2-4, 2005 (Basel, Switzerland), ASM International, 2005, p 1434-1440
3. C. Delbos, J. Fazilleau, V. Rat, J.F. Coudert, P. Fauchais, and B. Pateyron, Phenomena Involved in Suspension Plasma Spraying, Part 1: Suspension Injection and Behaviour, *Plasma Chem. Plasma Process.*, 2006, **26**(4), p 371-391
4. C. Delbos, J. Fazilleau, V. Rat, J.F. Coudert, P. Fauchais, and B. Pateyron, Phenomena Involved in Suspension Plasma Spraying, Part 2: Zirconia Particle Treatment and Coating Formation, *Plasma Chem. Plasma Process.*, 2006, **26**(4), p 393-414
5. H. Gleiter, Nanostructured Materials: Basic Concepts and Microstructure, *Acta Mater.*, 2000, **48**, p 1-29
6. D. Vollath and D.V. Szabó, Nanocoated Particles: A Special Type of Ceramic Powders, *Nanostruct. Mater.*, 1994, **4**(8), p 927-938
7. J. Freim and J. McKittrick, Microwave Sintering of Nanocrystalline γ-Al_2O_3, *Nanostruct. Mater.*, 1994, **4**(4), p 371-385
8. A. Rösler, G. Skillas, and S.E. Pratsinis, Nanopartikel – Material der Zukunft (Nano-Particles-Material for the Future), *Chemie in unserer Zeit*, 2001, **35**, p 32-41, in German
9. J. Karthikeyan, C.C. Berndt, S. Reddy, J.-Y. Wang, A.H. King, and H. Herman, Nanomaterials Deposits Formed by DC Plasma Spraying of Liquid Feedstocks, *J. Am. Ceram. Soc.*, 1998, **81**(1), p 121-128
10. P. Blazdell and S. Kuroda, Plasma Spraying of Submircron Ceramic Suspensions Using a Continuous Ink Jet Printer, *Surf. Coat. Technol.*, 2000, **123**, p 239-246
11. H. Gleiter, Nanostructured Materials: State of the Art and Perspectives, *Nanostruct. Mater.*, 1995, **6**, p 3-14
12. H. Gleiter, Nanostructured Materials, *Adv. Mater.*, 1992, **7/8**, p 474-480
13. H. Hahn and K.A. Padmanabhan, Mechanical Response of Nanostructured Materials, *Nanostruct. Mater.*, 1995, **6**(1), p 191-200
14. L. Xie, X. Ma, E.H. Jordan, N.P. Padture, D.T. Xiao, and M. Gell, Deposition Mechanisms of Thermal Barrier Coatings in the Solution Precursor Plasma Spray Process, *Surf. Coat. Technol.*, 2004, **177-178**, p 103-107
15. M. Gell, L. Xie, X. Ma, E.H. Jordan, and N.P. Padture, Highly Durable Thermal Barrier Coatings Made by the Solution Precursor Plasma Spray Process, *Surf. Coat. Technol.*, 2004, **177-178**, p 97-102
16. R. Siegert, *A Novel Process for the Liquid Feedstock Plasma Spray of Ceramic Coatings with Nanostructural Features*, Juelich Press, Germany, 2006, Jül-4205
17. L. Bianchi, A.C. Leger, M. Vardelle, A. Vardelle, and P. Fauchais, Splat Forming and Cooling of Plasma-Sprayed Zirconia, *Thin Solid films*, 1997, **305**, p 35-47